How much space is left for a new family of fermions?

Markus Bobrowski,[*] Alexander Lenz,[†] Johann Riedl,[‡] and Jürgen Rohrwild[§]

Institut für Theoretische Physik, Universität Regensburg, D-93040 Regensburg, Germany

We perform an exploratory study of the allowed parameter range for the CKM-like mixing of hypothetical quarks of a fourth generation. As experimental constraints we use the tree-level determinations of the 3×3 Cabibbo-Kobayashi-Maskawa (CKM) elements and flavor-changing neutral current (FCNC) processes (K, D, B_d, B_s mixing and the decay $b \to s\gamma$) under the assumption that the 4×4 CKM matrix is unitary. For the FCNCs we use some simplifying assumptions concerning the QCD corrections. Typically small mixing with the fourth family is favored; contrary to expectation, however, we find that also a quite large mixing with the fourth family is not yet excluded.

I. INTRODUCTION

Additional particle generations have been discarded for a long time. Recently this possibility (see [1] for a review) gained more interest. In contrast to many previous claims a fourth family is not in conflict with electroweak precision tests [2]; see also [3–5] for earlier works. The authors of [2] have shown that if the quark masses of the fourth generation fulfill the following relation:

$$m_{t'} - m_{b'} \approx \left(1 + \frac{1}{5}\ln\frac{m_H}{115 \text{ GeV}}\right) \times 55 \text{ GeV}, \quad (1.1)$$

the electroweak oblique parameters [6] are within the experimentally allowed regions. This also has the crucial side effect that a fourth generation softens the current Higgs bounds; see e.g. [7]. Moreover, an additional family might solve problems related to baryogenesis. First, it could lead to a sizable increase of the measure of *CP* violation; see [8]. Second it also would increase the strength of the phase transition; see [9]. In addition, the gauge couplings can be unified without invoking supersymmetry [10]. A new family also might cure certain problems in flavor physics; see e.g. [11–14] for some recent work and e.g. [15,16] for some early work on fourth generation effects on flavor physics. In view of the (re)start of the LHC, it is important not to exclude any possibility for new physics scenarios simply due to prejudices. In this work we, therefore, perform an exploratory study of the allowed parameter range for the CKM-like mixing of hypothetical quarks of a fourth generation. In Sec. II we

first describe the general parametrization used for the fourth generation Cabibbo-Kobayashi-Maskawa (CKM) matrix; next we explain the experimental constraints for the quark mixing. We then describe the numerical scan through the parameter space and finally we present the allowed parameter ranges for the mixing with an additional family. In Sec. III we perform a Taylor expansion of the 4×4 CKM matrix *à la* Wolfenstein, which makes the complicated general parametrization of V_{CKM4} much clearer; in particular, the possible hierarchy of the mixing is clearly visible. In Sec. IV we discuss some peculiar parameter ranges, which show huge deviations from current knowledge of the three-dimensional CKM matrix, and explain why these effects are not seen in the current CKM fits. Finally we conclude with an outlook on possible extensions of this exploratory study.

II. CONSTRAINTS ON V_{CKM4}

A. Parametrization of V_{CKM4}

Let the minimal standard model with three generations of fermions be denoted by SM3. The mixing between quarks is described by the unitary three-dimensional CKM matrix [17,18], which can be parametrized by three angles, θ_{12}, θ_{13}, and θ_{23} (θ_{ij} describes the strength of the mixing between the ith and jth family) and the *CP*-violating phase δ_{13}. The so-called standard parametrization of V_{CKM3} reads

$$V_{\text{CKM3}} = \begin{pmatrix} c_{12}c_{13} & s_{12}c_{13} & s_{13}e^{-i\delta_{13}} \\ -s_{12}c_{23} - c_{12}s_{23}s_{13}e^{i\delta_{13}} & c_{12}c_{23} - s_{12}s_{23}s_{13}e^{i\delta_{13}} & s_{23}c_{13} \\ s_{12}s_{23} - c_{12}c_{23}s_{13}e^{i\delta_{13}} & -c_{12}s_{23} - s_{12}c_{23}s_{13}e^{i\delta_{13}} & c_{23}c_{13} \end{pmatrix} \quad (2.1)$$

with

$$s_{ij} := \sin(\theta_{ij}) \quad \text{and} \quad c_{ij} := \cos(\theta_{ij}). \quad (2.2)$$

Extending the minimal standard model to include a fourth family of fermions (SM4) introduces at least 14 new pa-

[*]Markus.Bobrowski@physik.uni-regensburg.de
[†]Alexander.Lenz@physik.uni-regensburg.de
[‡]Johann.Riedl@physik.uni-regensburg.de
[§]Juergen.Rohrwild@physik.uni-regensburg.de

rameters. We do not take into account any correlations to the mixing matrix of the leptons. The seven parameters that are directly related to the quark sector are:

   (i) three additional angles in the CKM matrix, which we denote by θ_{14}, θ_{24}, and θ_{34},

   (ii) two additional *CP*-violating phases in the CKM matrix: δ_{14} and δ_{24},

  (iii) two quark masses of the fourth family: $m_{b'}$ and $m_{t'}$.

For the quark masses we have bounds from direct searches at Tevatron [19,20]

$$m_{b'} > 268 \text{ GeV}, \qquad m_{t'} > 256 \text{ GeV}. \tag{2.3}$$

In [21] it was claimed that in deriving these bounds implicit assumptions about the couplings of the fourth family have been made. Without these assumptions the mass bounds can be weaker. We investigate the following mass parameter range—taking into account the results of [2]

$$300 \text{ GeV} \leq m_{t'} \leq 650 \text{ GeV}, \tag{2.4}$$

$$m_{b'} = m_{t'} - 55 \text{ GeV}, \tag{2.5}$$

$$245 \text{ GeV} \leq m_{b'} \leq 595 \text{ GeV}. \tag{2.6}$$

Our goal is the determination of the current experimentally allowed ranges for the parameters θ_{14}, θ_{24}, θ_{34}, δ_{14}, and δ_{24}. For our numerical analysis we use an exact parametrization of the four-dimensional CKM matrix. The form suggested by Fritzsch and Plankl [22][1] and simultaneously by Harari and Leurer [23] turns out to be especially useful, because in the limiting case of vanishing mixing with the fourth family the standard parametrization of the 3×3 CKM matrix is restored. Moreover, this form of the matrix reveals a particularly convenient structure: the simplicity of the first row is advantageous because these elements are experimentally very well constrained, while the compact form of the last column simplifies the Taylor expansion presented in Sec. III,

$$V_{\text{CKM}}^{(4)} = \begin{pmatrix} c_{12}c_{13}c_{14} & c_{13}c_{14}s_{12} & c_{14}s_{13}e^{-i\delta_{13}} & s_{14}e^{-i\delta_{14}} \\ \begin{matrix} -c_{23}c_{24}s_{12} - c_{12}c_{24}s_{13}s_{23}e^{i\delta_{13}} \\ -c_{12}c_{13}s_{14}s_{24}e^{i(\delta_{14}-\delta_{24})} \end{matrix} & \begin{matrix} c_{12}c_{23}c_{24} - c_{24}s_{12}s_{13}s_{23}e^{i\delta_{13}} \\ -c_{13}s_{12}s_{14}s_{24}e^{i(\delta_{14}-\delta_{24})} \end{matrix} & \begin{matrix} c_{13}c_{24}s_{23} \\ -s_{13}s_{14}s_{24}e^{-i(\delta_{13}+\delta_{24}-\delta_{14})} \end{matrix} & c_{14}s_{24}e^{-i\delta_{24}} \\ \begin{matrix} -c_{12}c_{23}c_{34}s_{13}e^{i\delta_{13}} + c_{34}s_{12}s_{23} \\ -c_{12}c_{13}c_{24}s_{14}s_{34}e^{i\delta_{14}} \\ +c_{23}s_{12}s_{24}s_{34}e^{i\delta_{24}} \\ +c_{12}s_{13}s_{23}s_{24}s_{34}e^{i(\delta_{13}+\delta_{24})} \end{matrix} & \begin{matrix} -c_{12}c_{34}s_{23} - c_{23}c_{34}s_{12}s_{13}e^{i\delta_{13}} \\ -c_{12}c_{23}s_{24}s_{34}e^{i\delta_{24}} \\ -c_{13}c_{24}s_{12}s_{14}s_{34}e^{i\delta_{14}} \\ +s_{12}s_{13}s_{23}s_{24}s_{34}e^{i(\delta_{13}+\delta_{24})} \end{matrix} & \begin{matrix} c_{13}c_{23}c_{34} \\ -c_{13}s_{23}s_{24}s_{34}e^{i\delta_{24}} \\ -c_{24}s_{13}s_{14}s_{34}e^{i(\delta_{14}-\delta_{13})} \end{matrix} & c_{14}c_{24}s_{34} \\ \begin{matrix} -c_{12}c_{23}c_{34}s_{14}e^{i\delta_{14}} \\ +c_{12}c_{23}s_{13}s_{34}e^{i\delta_{13}} \\ +c_{23}c_{34}s_{12}s_{24}e^{i\delta_{24}} - s_{12}s_{23}s_{34} \\ +c_{12}c_{34}s_{13}s_{23}s_{24}e^{i(\delta_{13}+\delta_{24})} \end{matrix} & \begin{matrix} -c_{12}c_{23}c_{34}s_{24}e^{i\delta_{24}} + c_{12}s_{23}s_{34} \\ -c_{13}c_{24}c_{34}s_{12}s_{14}e^{i\delta_{14}} \\ +c_{23}s_{12}s_{13}s_{34}e^{i\delta_{13}} \\ +c_{34}s_{12}s_{13}s_{23}s_{24}e^{i(\delta_{13}+\delta_{24})} \end{matrix} & \begin{matrix} -c_{13}c_{23}s_{34} \\ -c_{13}c_{34}s_{23}s_{24}e^{i\delta_{24}} \\ -c_{24}c_{34}s_{13}s_{14}e^{i(\delta_{14}-\delta_{13})} \end{matrix} & c_{14}c_{24}c_{34} \end{pmatrix}.$$

$$\tag{2.7}$$

B. Experimental bounds

In this section we summarize the experimental constraints that have to be fulfilled by the quark mixing matrix. The elements of the 3×3 CKM matrix have been studied intensely for many years and precision data on most of them are available. In principle there are two different ways to determine the matrix elements. On the one hand, they enter charged weak decays already at tree level and a measurement of e.g. the corresponding decay rate provides direct information on the CKM elements (see e.g. [24] and references therein). We will refer to such constraints as *tree-level constraints*. On the other hand, processes involving a flavor-changing neutral current (FCNC) are forbidden at tree level and only come into play at loop level via the renowned penguin and box diagrams. These processes provide strong bounds, referred to as *FCNC constraints*, on the structure of the CKM matrix and its elements. In what follows we discuss the implications of these constraints in more detail.

Tree-level constraints for the CKM parameters: Since the (absolute) value of only one CKM element enters the theoretical predictions for weak tree-level decays, no

Glashow-Iliopoulos-Maiani mechanism (GIM) or unitary condition has to be assumed. By matching theory and experiment the matrix element can be extracted *independently* of the number of generations. Therefore, all tree-level constraints have the same impact on the 4×4 matrix as they have on the 3×3 one.

We take the Particle Data Group values [25] for our analysis:

	Absolute value	Relative error	Direct measurement from
V_{ud}	$0.974\,18 \pm 0.000\,27$	0.028%	nuclear beta decay
V_{us}	0.2255 ± 0.0019	0.84%	semileptonic K decay
V_{ub}	$0.003\,93 \pm 0.000\,36$	9.2%	semileptonic B decay
V_{cd}	0.230 ± 0.011	4.8%	semileptonic D decay
V_{cs}	1.04 ± 0.06	5.8%	(semi-)leptonic D decay
V_{cb}	0.0412 ± 0.0011	2.7%	semileptonic B decay
V_{tb}	>0.74		(single) top-production

In the following, we denote the absolute values in the table above as $|V_i| \pm \Delta V_i$. Next, we will discuss the bounds coming from FCNCs.

---

[1]In the original paper of Fritzsch and Plankl there is a typo in the element V_{cb}: c_{23} has to be replaced by s_{23}.

FCNC constraints: It is well known that FCNC processes give strong constraints on extensions of the standard model. In particular information about the CKM elements V_{tx} can be obtained by investigating B and K mixing. The mixing of the neutral mesons is described by box diagrams. As an example we show the box diagrams for B_d mixing:
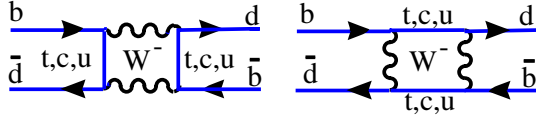
M_{12} encodes the virtual part of the box diagrams, which is very sensitive to new physics contributions. It is related to the mass difference of the neutral mesons via

$$\Delta M = 2|M_{12}|. \tag{2.8}$$

In the SM3 one obtains the following relations:

$$M_{12}^{K^0} \propto \eta_{cc}(\lambda_c^{K^0})^2 S_0(x_c) + 2\eta_{ct}\lambda_c^{K^0}\lambda_t^{K^0}S(x_c, x_t)$$
$$+ \eta_{tt}(\lambda_t^{K^0})^2 S_0(x_t), \tag{2.9}$$

$$M_{12}^{B_d} \propto \eta_{tt}(\lambda_t^{B_d})^2 S_0(x_t), \tag{2.10}$$

$$M_{12}^{B_s} \propto \eta_{tt}(\lambda_t^{B_s})^2 S_0(x_t), \tag{2.11}$$

with the Inami-Lim functions [26]

$$S_0(x) = \frac{4x - 11x^2 + x^3}{4(1-x)^2} - \frac{3x^3 \ln[x]}{2(1-x)^3}, \tag{2.12}$$

$$S(x, y) = xy\left[\frac{1}{y-x}\left(\frac{1}{4} + \frac{3}{2}\frac{1}{1-y} - \frac{3}{4}\frac{1}{(1-y)^2}\right)\ln[y]\right.$$
$$+ \frac{1}{x-y}\left(\frac{1}{4} + \frac{3}{2}\frac{1}{1-x} - \frac{3}{4}\frac{1}{(1-x)^2}\right)\ln[x]$$
$$\left. - \frac{3}{4}\frac{1}{1-x}\frac{1}{1-y}\right], \tag{2.13}$$

where $x_t = \frac{m_t^2}{M_W^2}$, the CKM elements

$$\lambda_x^{K^0} = V_{xd}V_{xs}^*, \qquad \lambda_x^{B_d} = V_{xd}V_{xb}^*, \qquad \lambda_x^{B_s} = V_{xs}V_{xb}^* \tag{2.14}$$

and the QCD corrections [27–29]

$$\eta_{cc} = 1.38 \pm 0.3, \qquad \eta_{ct} = 0.47 \pm 0.04,$$
$$\eta_{tt} = 0.5765 \pm 0.0065. \tag{2.15}$$

The full expressions for M_{12} can be found e.g. in [27,30].

In deriving these expressions unitarity (of the 3×3 matrix) was explicitly used, i.e.

$$\lambda_u^X + \lambda_c^X + \lambda_t^X = 0. \tag{2.16}$$

Moreover, in the B system the CKM elements of the different internal quark contributions are all roughly of the same size. Only the top contribution, which has by far the largest value of the Inami-Lim functions, survives. This is not the case in the K system. Here the top contribution is CKM suppressed, while the kinematically suppressed charm terms are CKM favored. Therefore, both have to be taken into account. More information about the mixing of neutral mesons can be found e.g. in [30,31].

For the mixing of neutral mesons we define the parameter Δ that quantifies the deviation from the standard model [30]

$$\Delta = \frac{M_{12}^{\mathrm{SM4}}}{M_{12}^{\mathrm{SM3}}} = |\Delta|e^{i\phi_\Delta}. \tag{2.17}$$

Going over to the SM4, we obtain

$$M_{12}^{K^0,\mathrm{SM4}} \propto \eta_{cc}(\lambda_c^{K^0})^2 S_0(x_c) + 2\eta_{ct}\lambda_c^{K^0}\lambda_t^{K^0}S(x_c, x_t)$$
$$+ \eta_{tt}(\lambda_t^{K^0})^2 S_0(x_t) + 2\eta_{ct'}\lambda_t^{K^0}\lambda_{t'}^{K^0}S(x_c, x_{t'})$$
$$+ 2\eta_{tt'}\lambda_t^{K^0}\lambda_{t'}^{K^0}S(x_t, x_{t'}) + \eta_{t't'}(\lambda_{t'}^{K^0})^2 S_0(x_{t'}), \tag{2.18}$$

$$M_{12}^{B_d,\mathrm{SM4}} \propto \eta_{tt}(\lambda_t^{B_d})^2 S_0(x_t) + \eta_{t't'}(\lambda_{t'}^{B_d})^2 S_0(x_{t'})$$
$$+ 2\eta_{tt'}\lambda_t^{B_d}\lambda_{t'}^{B_d}S(x_t, x_{t'}), \tag{2.19}$$

$$M_{12}^{B_s,\mathrm{SM4}} \propto \eta_{tt}(\lambda_t^{B_s})^2 S_0(x_t) + \eta_{t't'}(\lambda_{t'}^{B_s})^2 S_0(x_{t'})$$
$$+ 2\eta_{tt'}\lambda_t^{B_s}\lambda_{t'}^{B_s}S(x_t, x_{t'}). \tag{2.20}$$

Note that now also those CKM elements change that describe the mixing within the first three families! For simplicity we take the new QCD corrections to be

$$\eta_{t't'} = \eta_{tt'} = \eta_{tt} \quad \text{and} \quad \eta_{ct'} = \eta_{ct}. \tag{2.21}$$

In addition to the mixing quantities we also investigate the decay $b \to s\gamma$. To obtain the SM4 prediction for $b \to s\gamma$ one has to do the whole analysis of this decay without invoking the unitarity of the 3×3 CKM matrix, which is beyond the scope of this work. As an estimate of the effects of a fourth generation on $b \to s\gamma$, we simply define the ratio of the CKM structure times the corresponding Inami-Lim function $D_0'(x_t)$ [26][2]:

---

[2]The Inami-Lim function $D_0'(x_t)$ is proportional to the Wilson coefficient $C_{7\gamma}(M_W)$.

$$\Delta_{b\to s\gamma} := \frac{|\lambda_t^{SM4}|^2 D_0'(x_t)^2 + 2\,\mathrm{Re}(\lambda_t^{SM4}\lambda_{t'}^{SM4})D_0'(x_t)D_0'(x_{t'}) + |\lambda_{t'}^{SM4}|^2 D_0'(x_{t'})^2}{|\lambda_t^{SM3}|^2 D_0'(x_t)^2}, \tag{2.22}$$

with

$$D_0'(x) = -\frac{-7x + 5x^2 + 8x^3}{12(1-x)^3} + \frac{x^2(2-3x)}{2(1-x)^4}\ln[x]. \tag{2.23}$$

Parameters which give a value of $\Delta_{b\to s\gamma}$ close to 1 will also lead only to small deviations of $\Gamma(b\to s\gamma)^{SM4}/\Gamma(b\to s\gamma)^{SM3}$ from 1.

Currently, in particular, the hadronic uncertainties are under intense discussion; see e.g. [32]. Therefore, we use two sets of bounds for the allowed deviations from the SM3 values, which cover the possible range of uncertainties, a *conservative* and an *aggressive* one:

	Conservative bound	Aggressive bound
$|\Delta_{B_d}|$	1 ± 0.3	1 ± 0.1
$\phi_{B_d}^\Delta$	$0 \pm 10°$	$0 \pm 5°$
$|\Delta_{B_s}|$	1 ± 0.3	1 ± 0.1
$\phi_{B_s}^\Delta$	free	free
$\mathrm{Re}(\Delta_K)$	1 ± 0.5	1 ± 0.25
$\mathrm{Im}(\Delta_K)$	0 ± 0.3	0 ± 0.15
$\Delta_{b\to s\gamma}$	1 ± 0.15	1 ± 0.07

In [33] a very strong bound on $|V_{ub'}V_{cb'}|$ is extracted from D^0 mixing. We redo this analysis and confirm the conclusion of [33], although we are able to soften the bound by a factor of $\sqrt{3}$. The starting point is the mass difference in the neutral D^0 system, which can be expressed in terms of the parameter x_D

$$x_D = \frac{\Delta M_D}{\Gamma_D} = \frac{2|M_{12}^{D^0}|}{\Gamma_D}. \tag{2.24}$$

The Heavy Flavor Averaging Group [34] quotes for an experimental value of x_D

$$x_D = (0.811 \pm 0.334) \cdot 10^{-2}. \tag{2.25}$$

Starting with the expression for the box diagram and using the unitarity condition $\lambda_d^{D^0} + \lambda_s^{D^0} + \lambda_b^{D^0} + \lambda_{b'}^{D^0} = 0$ (with $\lambda_x^{D^0} = V_{cx}V_{ux}^*$), we obtain

$$\begin{aligned} M_{12}^{D^0} \propto\ & \lambda_s^2 S_0(x_s) + 2\lambda_s\lambda_b S(x_s, x_b) + \lambda_b^2 S_0(x_b) + \mathrm{LD} \\ & + 2\lambda_s\lambda_{b'}S(x_s, x_{b'}) + 2\lambda_b\lambda_{b'}S(x_b, x_{b'}) + \mathrm{LD} \\ & + \lambda_{b'}^2 S_0(x_{b'}), \end{aligned} \tag{2.26}$$

where the proportionality constant is

$$\frac{G_F^2 M_W^2 M_D}{12\pi^2} f_D^2 B_D \eta(m_c, M_W). \tag{2.27}$$

Lubicz and Tarantino [35] gave a survey of recent lattice data and provided an averaged decay constant $f_{D^0} = 212 \pm 14$ MeV and bag parameter $B = 0.85 \pm 0.09$. In order to compare with the results of [33], we use only the leading-order expression of the QCD correction factor η,

$$\eta(m_c, M_W) \equiv \left(\frac{\alpha_s^{(4)}(m_b)}{a_s^{(4)}(m_c)}\right)^{6/25}\left(\frac{\alpha_s^{(5)}(M_W)}{\alpha_s^{(5)}(m_b)}\right)^{6/23} \simeq 0.74. \tag{2.28}$$

The first line of (2.26) corresponds to the pure SM3 contribution, the third line is due to contributions of the heavy fourth generation and the second line is a term arising when SM3 and b' contributions mix:

$$M_{12}^{D^0} = M_{12,SM3}^{D^0} + M_{12,Mix}^{D^0} + M_{12,b'}^{D^0}. \tag{2.29}$$

The perturbative short-distance contribution to $M_{12,SM3}^{D^0}$ is numerically very small. The first two terms in the first line of (2.26) are kinematically suppressed and the third term suffers a Cabibbo suppression caused by a CKM factor of order $\mathcal{O}(10^{-8})$, such that an operator-product expansion (OPE)-based standard model calculation yields values of about $x \approx 4 \cdot 10^{-5}$. The order of magnitude of this result complies with early estimates for x_D, which relied merely on perturbation theory calculations and ranged between roughly 10^{-6} [36] and 10^{-4} [37]. It has often been pointed out that in the case of charmed mesons a substantial enhancement of the mass and width differences has possibly to be attributed to long-distance (LD) effects, which cannot be calculated perturbatively; see e.g. [38–42]. The quoted predictions usually rely on exclusive estimates of decay widths; they can be considerably increased by nearby resonances. Typical results are in the range of $x_D, y_D \simeq 10^{-4} \dots 10^{-3}$, which almost reach the order of magnitude of the experimental values. Bigi and Uraltsev [38] argue that, albeit the leading $1/m_c$ contributions are negligibly small and the validity of duality is very questionable, operators of higher dimension might lead to values of x_D, y_D up to $5 \cdot 10^{-3}$ in the framework of the standard OPE techniques, what is already very close to the experimental values. The short-distance terms of the mixed part $M_{12,Mix}^{D^0}$ are numerically at most as large as the short-distance part of the pure SM3 contribution. The s-quark term of the mixed part is about twice the b-quark term and it might also be affected by large long-distance effects. For $M_{12,b'}^{D^0}$ the OPE is expected to work perfectly and no sizable unknown nonperturbative effects are likely to appear. Numerically this term can be much larger than the short-distance parts of the SM3 and the mixed contribution. The idea of [33] was to neglect all terms in $M_{12}^{D^0}$, except $M_{12,b'}^{D^0}$, and to equate this term with the experimental number for x_D. Following this strategy we reproduce the bounds given in [33]. We think, however, that it is not completely excluded that there might be large nonperturbative contributions to both $M_{12,SM3}^{D^0}$ and $M_{12,Mix}^{D^0}$, each of the size of the experimental value of x_D. This would enhance the possible range for $M_{12,b'}^{D^0}$ by a factor of up to 3 compared to [33]. Allowing this possibility we obtain the following, very

conservative bounds on $|V_{ub'}V_{cb'}|$; see also Fig. 1:

$$|V_{ub'}V_{cb'}| \le \begin{cases} 0.003\,95 & \text{for } m_{b'} = 200 \text{ GeV,} \\ 0.002\,90 & \text{for } m_{b'} = 300 \text{ GeV,} \\ 0.001\,93 & \text{for } m_{b'} = 500 \text{ GeV.} \end{cases} \quad (2.30)$$

Even as we were able to soften the bound of [33] by a factor $\sqrt{3}$, D^0 mixing is still by far the strongest direct constraint on $|V_{ub'}V_{cb'}|$. We take the values of Eq. (2.30) for our conservative bounds, while we take the results of [33] as the aggressive ones.

C. Scan through the mixing parameters

Subsequently, we will describe the scan through the nine-dimensional parameter space of the 4×4 mixing matrix and the mass regions for $m_{t'}$ and test whether the experimental constraints on quark mixing are fulfilled. For this purpose we use the exact parametrization of V_{CKM4} described in Sec. II A, Eq. (2.7). For the allowed ranges—especially on the new parameters related to the fourth generation—it is crucial how to treat the errors of the tree-level bounds. We have decided to study two different treatments of the error ranges. We adopt a conservative and an aggressive set of bounds. In both the conservative and the aggressive case, the bound on V_{tb} is assumed to be hard. We enforce each of the six other tree-level constraints to be individually fulfilled at the 2σ level, i.e. our CKM matrix element $V_{\text{CKM4},i}$ has to be in the range

$$|V_i| - 2\Delta V_i < |V_{\text{CKM4},i}| < |V_i| + 2\Delta V_i.$$

Additionally, in order to have a measure for the deviation from the central values of the tree-level bounds, we define a χ^2 per degree of freedom (d.o.f.) as

$$\chi^2/\text{d.o.f.} = \frac{1}{n} \sum_{i=ud,us,ub,cd,cs,cb} \left(\frac{|V_{\text{CKM4},i}| - |V_i|}{\Delta V_i} \right)^2,$$

where $n = 6$ is the number of considered degrees of freedom. For the conservative constraints we call for $\chi^2/\text{d.o.f.} < 2$ and for the aggressive ones for $\chi^2/\text{d.o.f.} <$
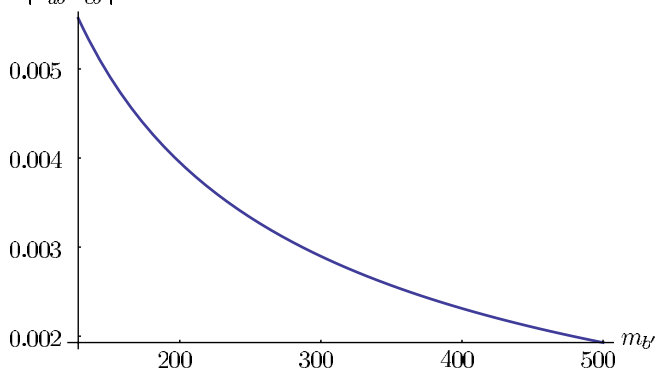

FIG. 1 (color online). Bound on $|V_{ub'}V_{cb'}|$ determined from the measurement of D^0 mixing in dependence on the mass of the b' quark.

TABLE I. Preselection bounds resulting from tree-level determinations of the CKM elements for the angles of the quark mixing matrix.

	Θ_{12}	Θ_{13}	Θ_{23}	Θ_{14}	Θ_{24}	Θ_{34}
Minimum value	0.222	0.0033	0.038	0	0	0
Maximum value	0.232	0.0048	0.046	0.069	0.19	0.8

0.5. The choice for the aggressive bounds has been inspired by the fact, that one obtains for the best CKM3 fit given by the Particle Data Group $\chi^2/\text{d.o.f.} = 0.4$. In other words, with our aggressive constraints on the tree-level bounds, we do not want to violate the tree-level constraints significantly more than the CKM3 fit. From the tree-level constraints and careful checks with larger parameter ranges, we find that we safely restrict ourselves to the ranges given in Table I. The phases δ_{13}, δ_{14}, and δ_{24} have been left unconstrained. The mass $m_{t'}$ was scanned from 300 to 650 GeV as described in Eq. (2.4). In this ten-dimensional space we generate more than $2 \cdot 10^{10}$ randomly distributed points and check whether they meet the tree-level and FCNC constraints given above.[3] To this end, we first employ the conservative set of bounds. We only store parameter sets which satisfy these bounds—only 12 817 846 data sets remain afterward. The aggressive bounds are established by subsequent reduction of the conservative data, leaving only 150 763 points. To give an impression how important each constraint is under the assumption of our preselection, we have used each bound individually and switched off the others.

We obtain the following result: already the tree-level constraints reduce the allowed parameter space dramatically.

Only 13% of the randomly created points in the preselected parameter space actually pass the combined tree-level bounds. The strongest restrictions stem from $|V_{ud}|$, which is constrained to a relative error of only 0.028%. As a consequence, due to $V_{ud} = c_{12}c_{13}c_{14}$, the allowed ranges for θ_{12} and θ_{14} are quite small (θ_{13} is tiny; its precise value does not play a major role for $|V_{ud}|$). Another important contribution to the rejection rate stems from the χ^2 bound. The FCNC constraints are even more restrictive, e.g. even in the conservative case only 1.5% of the configurations pass the Δ_{B_d} bound; see Table II for more details.

Having done our scan, we have found no accepted parameter sets beyond the following ranges:

	Conservative bound	Aggressive bound
θ_{14}	≤ 0.0535	≤ 0.0364
θ_{24}	≤ 0.144	≤ 0.104
θ_{34}	≤ 0.737	≤ 0.736
δ_{14}	free	free
δ_{24}	free	free

---

[3]A similar strategy with 60 000 points was pursued in [43].

TABLE II. The impact of the (conservative) constraints on the five flavor-changing neutral currents. The second row gives the probability that a random point in the configuration space fulfills the FCNC bounds. The third row corresponds to the probability that a set of angles and phases that is in agreement with tree-level bounds also passes the FCNC bound.

	Δ_{K^0}	Δ_{B_d}	Δ_{B_s}	$\Delta_{b \to s\gamma}$	D^0 mixing
Without tree-level bounds	21%	1.5%	29%	16%	46%
With tree-level bounds	27%	2.1%	32%	20%	62%

This is one of the main results of this work. Typically small mixing with the fourth family is favored, but there is still room for sizable effects. To further explain our results, we note that not all combinations for these new parameters are allowed. Apart from studying the allowed parameter regions in a one-dimensional projection as presented above, we show correlations of selected input parameter pairs. Figures 2–6 correspond to the θ_{14}-θ_{24}, θ_{24}-θ_{34}, δ_{13}-δ_{14}, δ_{14}-δ_{24}, and θ_{12}-θ_{14} planes. We divide each direction (i.e. x axis and y axis) of each plot in 300 steps. So that the total picture consists of $300 \times 300 = 90\,000$ color encoded unit squares. In the upper panels the color encoding counts the number of accepted sets in each unit square. As a large range is covered, we chose to plot Figs. 2–4 and 6 logarithmically. The number next to the color scale then gives the natural logarithm of the number of accepted sets per

unit square. As the distribution in the δ_{14}-δ_{24} plane is somewhat more homogeneous we choose a linear scale for Fig. 5. The upper left panel in each plot is for the conservative bounds and the upper right one for the aggressive ones. In the lower panels we present the mass dependence of the allowed parameter ranges. Obviously, there is a nontrivial influence of the t' mass on these ranges. The left panel corresponds to the conservative and the right panel to the aggressive bounds. The plots show the distribution of the accepted points in the three mass regions indicated in the plot. In most cases a lower mass results in a larger allowed parameter space. But there are also nontrivial exceptions, cf. Fig. 3. Especially the restriction due to the D^0 mixing bound (as described in Sec. II B) can be seen clearly as hyperbolic cuts in Fig. 2. The mass dependence in Fig. 5 is not shown as in each case the whole square is filled.

In Figs. 7–9, the distribution of the accepted points in the complex $\Delta_{[K^0, B_d, B_s]}$ plane is shown. As above, in each plot the left panel corresponds to the conservative constraints and the right panel to the aggressive ones. For Δ_{K^0} and Δ_{B_s} a logarithmic scale is chosen and for Δ_{B_d} a linear one, corresponding to the observation that for B_d the points are somewhat more homogeneously distributed than in the other two cases. This corresponds to the observation that the acceptance rate of the B_d bound is very low, only 2.1% after tree-level bounds, as shown in Table II. The reason for
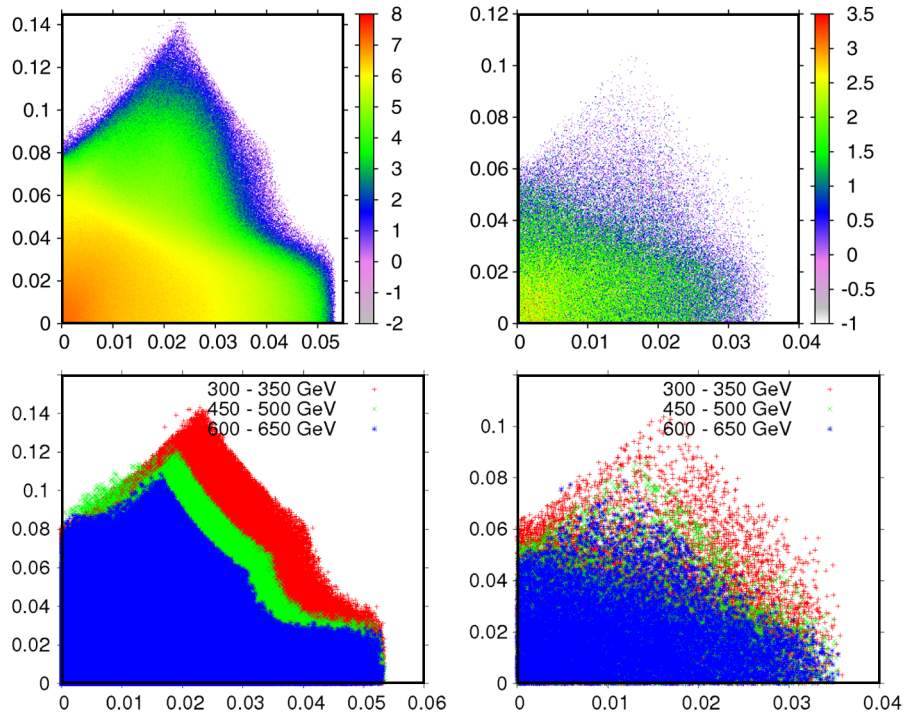

FIG. 2 (color online). In the upper left and upper right panel, the allowed parameter ranges for θ_{14} on the x axis and θ_{24} on the y axis are shown for the conservative and the aggressive bounds, respectively. The color encodes the relative occurrence as explained in the text. In the lower left and right panels the allowed parameter range is shown in dependence on the t' mass for three different mass ranges for the conservative and aggressive bounds, respectively.
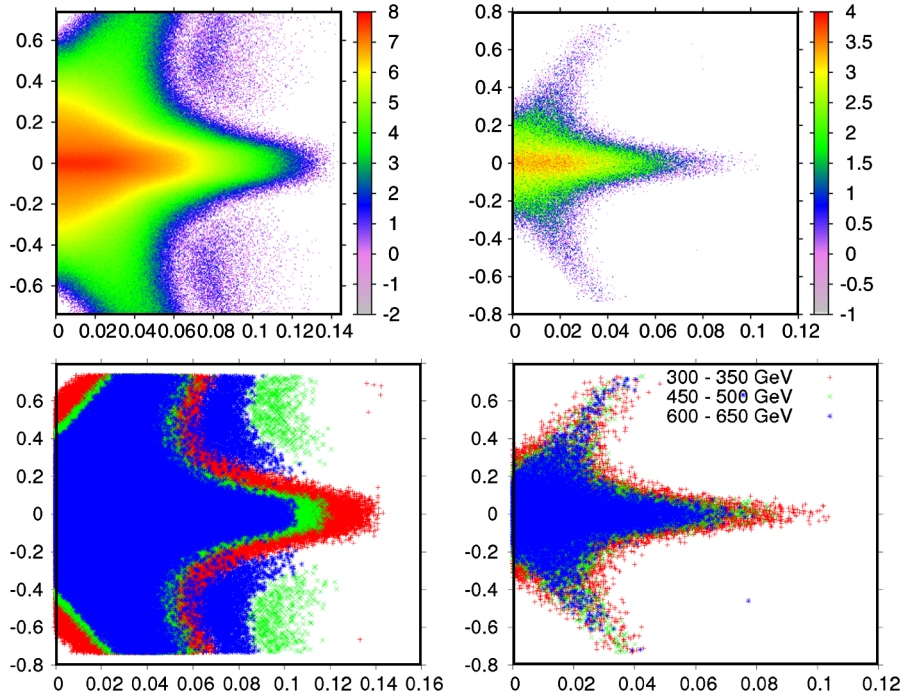
FIG. 3 (color online).   The allowed parameter ranges in θ_{24} and θ_{34}. For further explanation, see the caption of Fig. 2.

this behavior is the following: Enforcing only the tree-level bounds and unitarity Δ_{B_d} can take values up to 50 times the standard model prediction. Therefore, the stringent experimental bounds on Δ_{B_d} put forward severe restrictions on the allowed parameter range.

In Fig. 10 the dependence on the t' mass for the three FCNC observables is shown. Only for Δ_{B_s}, a strong influence of the mass on the results is seen. For Δ_{K^0} the influence is still perceivable but rather weak, whereas Δ_{B_d} seems to be almost independent of $m_{t'}$. The complex
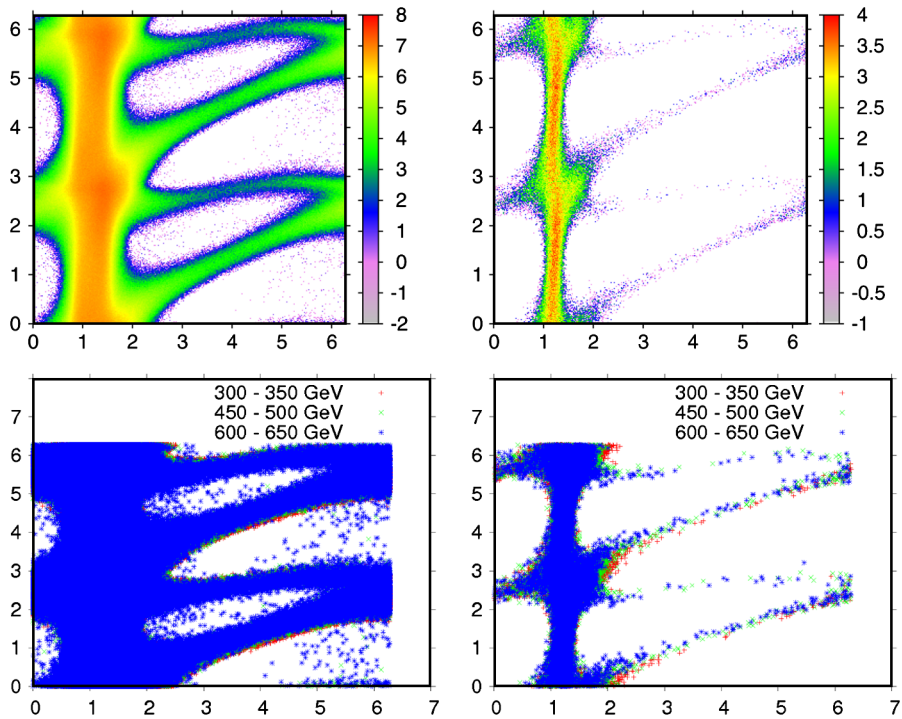
FIG. 4 (color online).   The allowed parameter ranges in δ_{13} and δ_{14}. For further explanation, see the caption of Fig. 2.
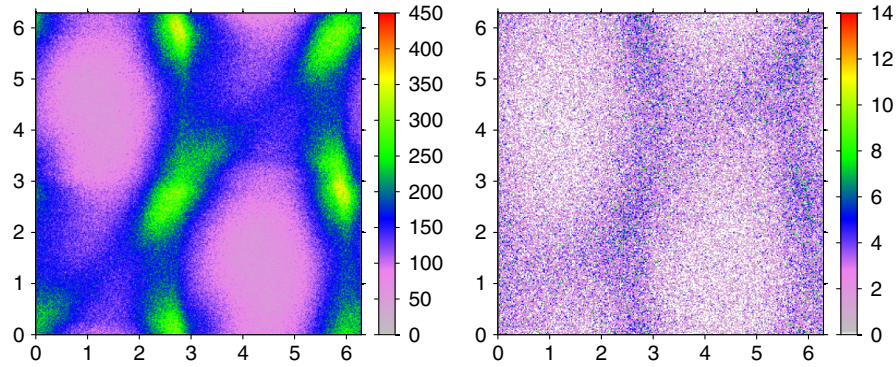
FIG. 5 (color online). The allowed parameter ranges in δ_{14} and δ_{24}. For further explanation, see the caption of Fig. 2. Here, the mass dependence is not explicitly shown, as all combinations are allowed for each mass $m_{t'}$.
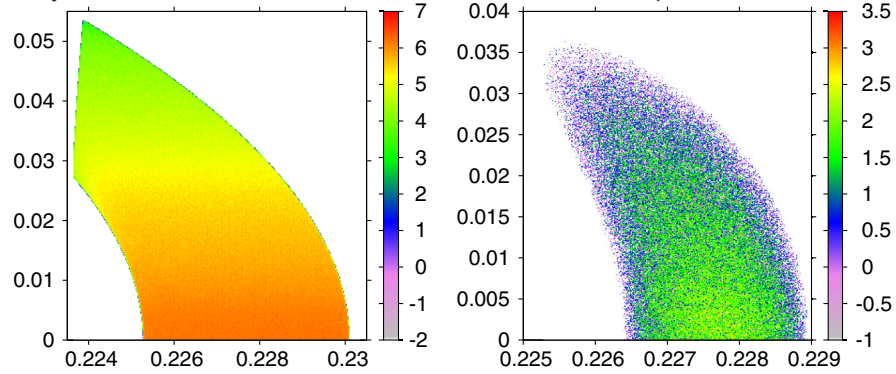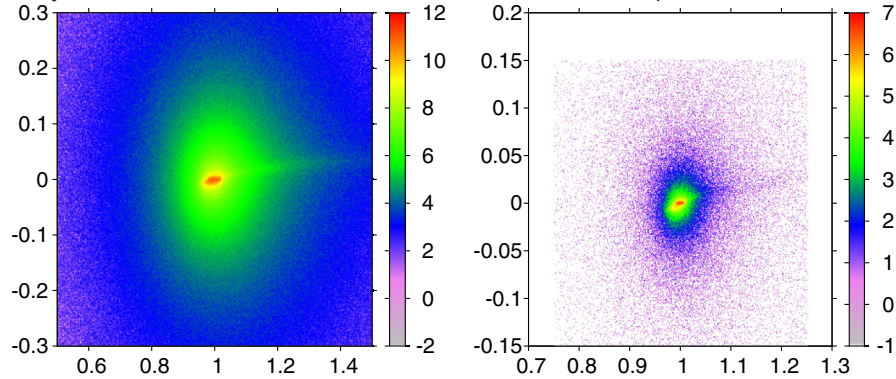

FIG. 6 (color online). The allowed parameter ranges in θ_{12} and θ_{14}. For further explanation, see the caption of Fig. 2. Here, the mass dependence is not explicitly shown, as all combinations are allowed for each mass $m_{t'}$.

FIG. 7 (color online). The results for Δ_{K^0} shown in the complex plane (real part on the x axis and imaginary part on the y axis): in the left panel for the conservative bounds and in the right panel for the aggressive ones.
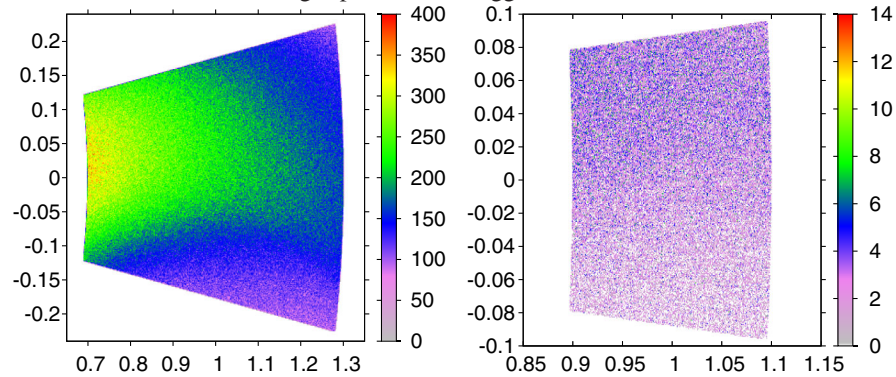

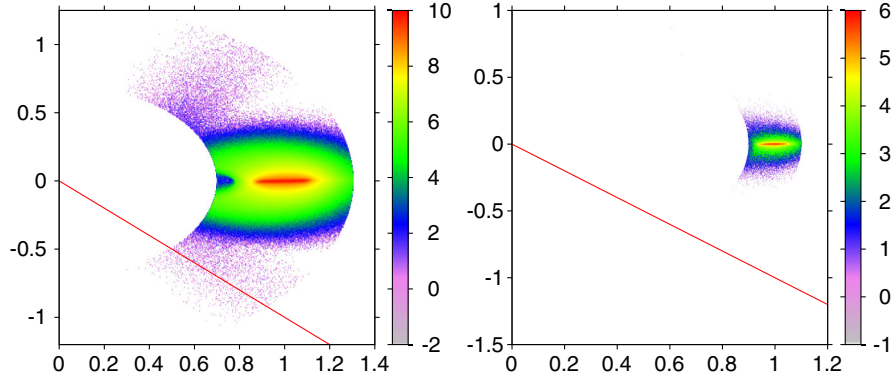FIG. 8 (color online). The results for Δ_{B_d} as described in the caption of Fig. 7.

FIG. 9 (color online).   The results for Δ_{B_s} as described in the caption of Fig. 7. The solid line represents a Φ_s angle of $-45°$ which is hinted by recent experiments.
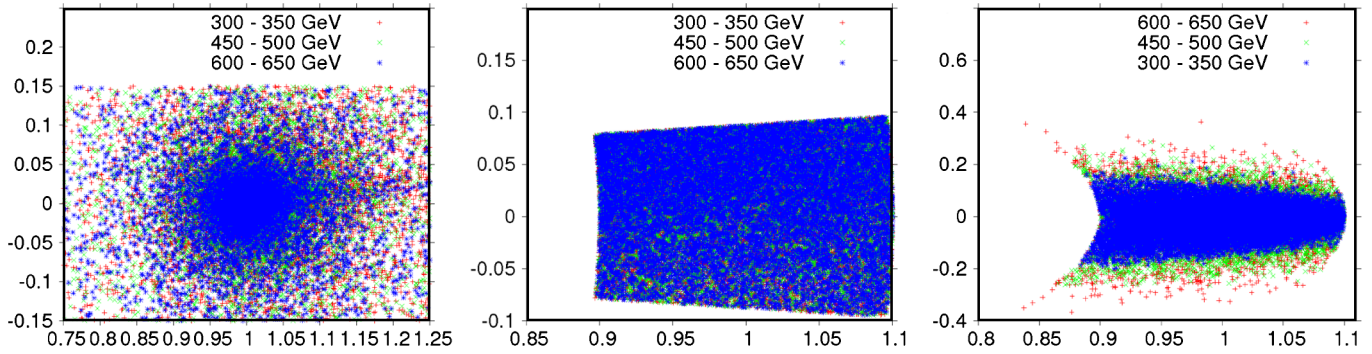

FIG. 10 (color online).   The $m_{t'}$ dependence of the FCNC Δs: from left to right Δ_K, Δ_{B_d}, and Δ_{B_s}.
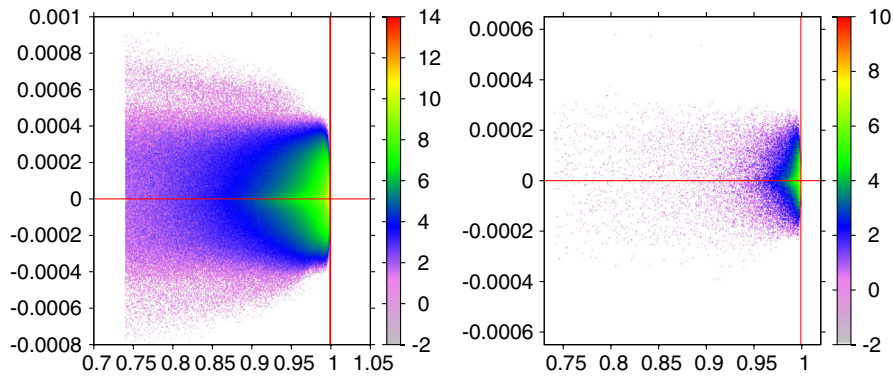

FIG. 11 (color online).   The results for V_{tb} as described in the caption of Fig. 7. The solid crossed lines give the value for CKM3.
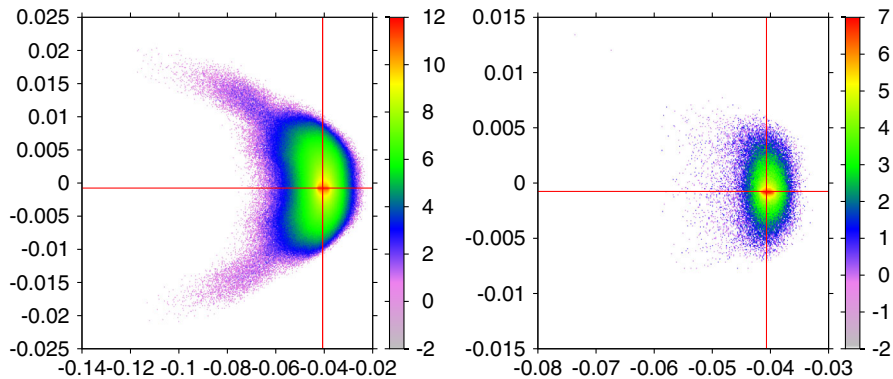

FIG. 12 (color online).   The results for V_{ts} as described in the caption of Fig. 7. The solid crossed lines give the value for CKM3.
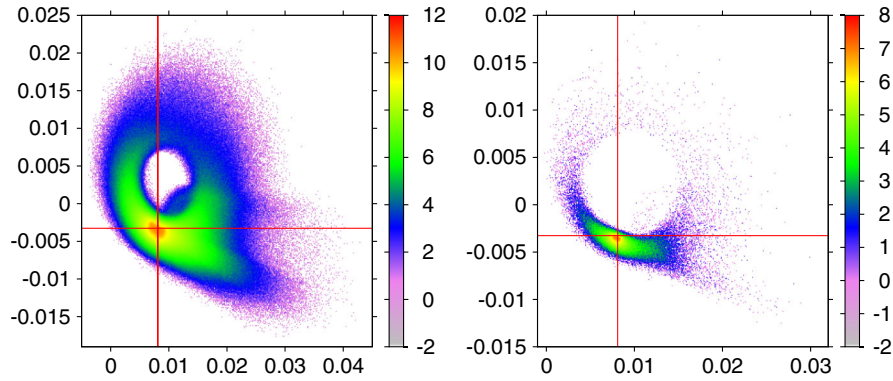
FIG. 13 (color online). The results for V_{td} as described in the caption of Fig. 7. The solid crossed lines give the value for CKM3. The peculiar ring structure already arises after enforcing unitarity and tree-level bounds.
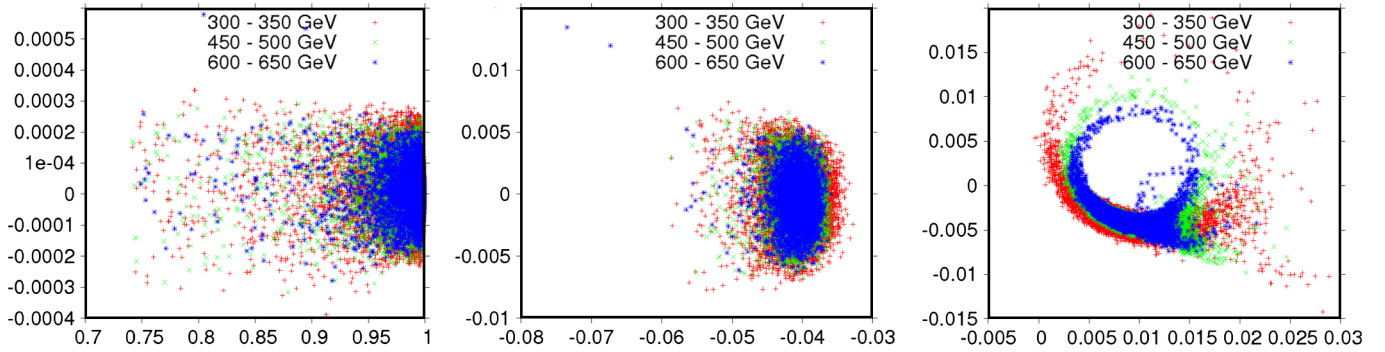

FIG. 14 (color online). The dependence of the CKM elements V_{tb} (left panel), V_{ts} (middle panel), and V_{td} (right panel) on the mass region.

Δ_B planes are particularly interesting since there might be some hints on new physics effects in B_s mixing; see [30,44] and the Web updates of [45]. In [30] a visualization of the combination of the mixing quantities ΔM_s, $\Delta\Gamma_s$, a_{sl}^s, which are known to next-to-leading-order QCD [27,46–48] and of direct determinations of Φ_s in the complex Δ plane was suggested. Combining recent measurements [49,50] for the phase Φ_s one obtains a deviation from the tiny SM prediction [30] in the range of 2 to 3σ:

   (i) HFAG: 2.2σ [49],
   (ii) CKM-Fitter: $2.1\dots2.5\sigma$ [51,52],
   (iii) UT-Fit: 2.9σ [44].

The central values of these deviations cluster around

$$\Phi_s \approx -45°. \qquad (2.31)$$

As can be read from Fig. 9 sizable values for Φ_s can also be obtained in scenarios with additional fermions. Such large values for Φ_s are not favored but they are possible. An enhancement of Φ_s to large negative values by contributions of a fourth family was first discussed in [12].

In Figs. 11–13 we present the values for the CKM matrix elements V_{tb}, V_{ts}, and V_{td} in the complex plane. As in the Figs. 7–9 the left panel is for the conservative case and the right panel for the aggressive one. For comparison the SM3 expectations are given as thin red lines. Obviously, large deviations from the SM expectations are possible. The

peculiar structure of the allowed range for V_{td} arises already after imposing unitarity and tree-level constraints. The nontrivial mass dependence for the aggressive case is shown in Fig. 14. In Fig. 15 we show the mass dependence of the acceptance rate. The number of accepted data points per 50 GeV normalized to the total number of accepted
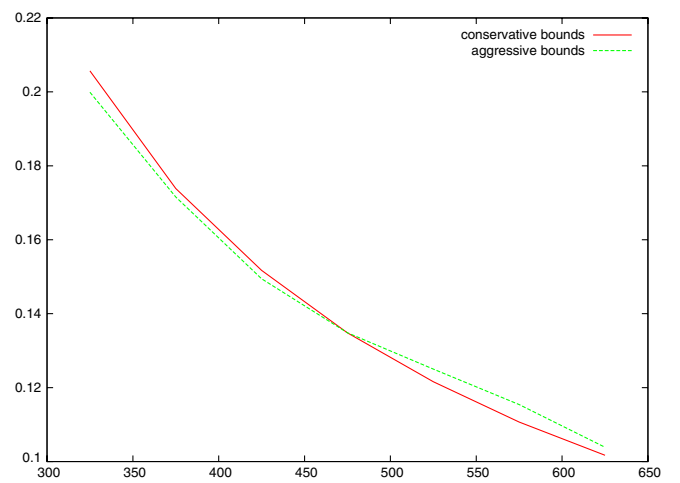

FIG. 15 (color online). Relative distribution of the accepted 12 817 846 and 150 763 points using the conservative and the aggressive bounds, respectively. The relative occurrence is shown on the y axis and $m_{t'}$ on the x axis.

points is plotted versus the mass $m_{t'}$. It can be seen that the acceptance rate reduces with growing t' mass. Because our test points are randomly distributed over the whole mass region, an acceptance rate independent from the mass would feature a constant functional behavior; this is clearly not observed. One can also notice a small difference in the acceptance rate for conservative and aggressive bounds.

III. TAYLOR EXPANSION OF V_{CKM4}

The hierarchy of the mixing between the three quark families can be visualized by the Wolfenstein parametrization [53]. It is obtained from the standard parametrization by performing a Taylor expansion in the small CKM element $V_{us} \approx 0.2255$. Following [54] we define

$$V_{ub} = s_{13}e^{-i\delta_{13}} =: A\lambda^4(\tilde{\rho} + i\tilde{\eta}), \tag{3.1}$$

$$V_{us} = s_{12}(1 + \mathcal{O}(\lambda^8)) =: \lambda, \tag{3.2}$$

$$V_{cb} = s_{23}(1 + \mathcal{O}(\lambda^8)) =: A\lambda^2. \tag{3.3}$$

Note that due to historical reasons the element V_{ub} is typically defined to be of order λ^3, while it turned out that it is numerically of order λ^4:

$$|V_{ub}| = 0.003\,93 = 1.51\lambda^4 = 0.34\lambda^3. \tag{3.4}$$

Up to terms of order λ^6 the Taylor expansion of the CKM matrix assumes the form

$$V_{CKM3} = \begin{pmatrix} 1 - \frac{\lambda^2}{2} - \frac{\lambda^4}{8} - \frac{\lambda^6}{16} & \lambda & A\lambda^4(\tilde{\rho} - i\tilde{\eta}) \\ -\lambda + A^2\frac{\lambda^5}{2} - A^2\lambda^6(\tilde{\rho} + i\tilde{\eta}) & 1 - \frac{\lambda^2}{2} - \frac{\lambda^4}{8} - \frac{A^2\lambda^4}{2} + \frac{A^2\lambda^6}{4} - \frac{\lambda^6}{16} & A\lambda^2 \\ A\lambda^3 - A\lambda^4(\tilde{\rho} + i\tilde{\eta}) & -A\lambda^2(1 - \frac{\lambda^2}{2} + \lambda^3(\tilde{\rho} + i\tilde{\eta}) - \frac{\lambda^4}{8}) & 1 - \frac{A^2\lambda^4}{2} \end{pmatrix}. \tag{3.5}$$

This result can be obtained from the standard Wolfenstein parametrization by replacing

$$\rho =: \lambda\tilde{\rho}, \qquad \eta =: \lambda\tilde{\eta}. \tag{3.6}$$

For the case of four generations we have to determine first the possible size, i.e. the power in λ of the new CKM matrix elements. With the results of the previous section we obtain:

	Conservative bound	Aggressive bound
$|V_{ub'}|$	$\leq 0.0535 \approx 1.05\lambda^2$	$\leq 0.0364 \approx 0.7\lambda^2 \approx 3.2\lambda^3$
$|V_{cb'}|$	$\leq 0.144 \approx 0.6\lambda^1 \approx 2.8\lambda^2$	$\leq 0.104 \approx 0.46\lambda^1 \approx 2\lambda^2$
$|V_{tb'}|$	$\leq 0.672 \approx 3.0\lambda^1$	$\leq 0.671 \approx 3.0\lambda^1$

We propose a parametrization of these matrix elements that manifestly respects the above bounds:

(i) For the mixing of first and fourth family we define

$$V_{ub'} = s_{14}e^{-i\delta_{14}} := \lambda^2(x_{14} - iy_{14})$$

$$\Rightarrow s_{14} = \lambda^2\sqrt{x_{14}^2 + y_{14}^2}$$

$$\Rightarrow c_{14} = 1 - \lambda^4\frac{x_{14}^2 + y_{14}^2}{2} + O(\lambda^8), \tag{3.7}$$

which is a good estimate for both, conservative and aggressive bounds, since the parameters x_{14} and y_{14} can safely be assumed to be smaller than 1.

(ii) The estimate for the matrix element $V_{cb'}$ is more complicated. The conservative bound suggests a size of order λ, whereas the aggressive bound might justify a leading power λ^2. In what follows we opt

for the more solid $\mathcal{O}(\lambda)$ variant. We define

$$V_{cb'} = c_{14}s_{24}e^{-i\delta_{24}} := (x_{24} - iy_{24})\lambda^1$$

$$\Rightarrow s_{24}e^{-i\delta_{24}} = (x_{24} - iy_{24})\lambda + \frac{1}{2}(x_{14}^2 + y_{14}^2)$$
$$\times (x_{24} - iy_{24})\lambda^5 + O(\lambda^7)$$

$$\Rightarrow c_{24} = 1 + \frac{1}{2}(-x_{24}^2 - y_{24}^2)\lambda^2 - \frac{1}{8}(x_{24}^2 + y_{24}^2)^2\lambda^4$$
$$+ \frac{1}{6}\left(\frac{3}{8}(-x_{24}^2 - y_{24}^2)^3 + 3(-x_{14}^2 - y_{14}^2)\right.$$
$$\left. \times (x_{24}^2 + y_{24}^2)\right)\lambda^6 + O(\lambda^7). \tag{3.8}$$

(iii) Finally, the element $|V_{tb'}|$ is not constrained to be significantly smaller than 1 and we cannot restrict the mixing angle Θ_{34}. Thus, we keep cosine c_{34} and sine s_{34} in the expansion.

It is obvious that already at $\mathcal{O}(\lambda^6)$ the expansion gets confusing; see (3.8). For the Taylor expansion to provide an intuitive picture of the hierarchy of the elements and the still possible effects of the mixing with the fourth generation we want to keep the matrix clearly arranged. Therefore we expand the CKM4 matrix up to and including order λ^4. The matrix elements take the form

$$V_{ud} = 1 - \frac{\lambda^2}{2} - \frac{1}{8}(4x_{14}^2 + 4y_{14}^2 + 1)\lambda^4, \qquad V_{us} = \lambda,$$
$$V_{ub} = A(\tilde{\rho} - i\tilde{\eta})\lambda^4, \qquad V_{ub'} = (x_{14} - iy_{14})\lambda^2, \tag{3.9}$$

$$V_{cd} = -\lambda + \frac{1}{2}(x_{24} - iy_{24})(-2x_{14} + x_{24} - 2iy_{14} + iy_{24})\lambda^3,$$

$$V_{cs} = 1 - \frac{1}{2}(x_{24}^2 + y_{24}^2 + 1)\lambda^2 + \frac{1}{8}(-x_{24}^4 - 2(y_{24}^2 - 1)x_{24}^2 - 8iy_{14}x_{24} - y_{24}^4 - 4A^2 + 2y_{24}^2 - 8x_{14}(x_{24} - iy_{24})$$
$$- 8y_{14}y_{24} - 1)\lambda^4,$$

$$\qquad\qquad (3.10)$$

$$V_{cb} = A\lambda^2, \qquad V_{cb'} = (x_{24} - iy_{24})\lambda,$$

$$V_{td} = s_{34}(-x_{14} + x_{24} - i(y_{14} - y_{24}))\lambda^2 + Ac_{34}\lambda^3 + \frac{1}{2}[A(-2i\tilde{\eta} - 2\tilde{\rho})c_{34} + s_{34}(x_{14} + iy_{14})(x_{24}^2 + y_{24}^2 + 1)]\lambda^4,$$

$$V_{ts} = -s_{34}(x_{24} + iy_{24})\lambda - Ac_{34}\lambda^2 + \frac{1}{2}s_{34}(-2x_{14} + x_{24} - 2iy_{14} + iy_{24})\lambda^3 - \frac{1}{2}[Ac_{34}(x_{24}^2 + y_{24}^2 - 1)]\lambda^4,$$

$$\qquad\qquad (3.11)$$

$$V_{tb} = c_{34} - As_{34}(x_{24} + iy_{24})\lambda^3 - \frac{1}{2}(A^2 c_{34})\lambda^4,$$

$$V_{tb'} = s_{34} - \frac{1}{2}[s_{34}(x_{24}^2 + y_{24}^2)]\lambda^2 - \frac{1}{8}[s_{34}(x_{24}^4 + 2y_{24}^2 x_{24}^2 + y_{24}^4 + 4x_{14}^2 + 4y_{14}^2)]\lambda^4,$$

$$V_{t'd} = c_{34}[-x_{14} + x_{24} - i(y_{14} - y_{24})]\lambda^2 - As_{34}\lambda^3 + \frac{1}{2}[2A(i\tilde{\eta} + \tilde{\rho})s_{34} + c_{34}(x_{14} + iy_{14})(x_{24}^2 + y_{24}^2 + 1)]\lambda^4,$$

$$V_{t's} = -c_{34}(x_{24} + iy_{24})\lambda + As_{34}\lambda^2 + \frac{1}{2}c_{34}(-2x_{14} + x_{24} - 2iy_{14} + iy_{24})\lambda^3 + \frac{1}{2}As_{34}(x_{24}^2 + y_{24}^2 - 1)\lambda^4,$$

$$\qquad\qquad (3.12)$$

$$V_{t'b} = -s_{34} - Ac_{34}(x_{24} + iy_{24})\lambda^3 + \frac{1}{2}A^2 s_{34}\lambda^4,$$

$$V_{t'b'} = c_{34} - \frac{1}{2}[c_{34}(x_{24}^2 + y_{24}^2)]\lambda^2 - \frac{1}{8}[c_{34}(x_{24}^4 + 2y_{24}^2 x_{24}^2 + y_{24}^4 + 4x_{14}^2 + 4y_{14}^2)]\lambda^4.$$

The terms $s_{34}(-x_{14} + x_{24} - i(y_{14} - y_{24}))\lambda^2$ in V_{td} and $-s_{34}(x_{24} + iy_{24})\lambda$ in V_{ts} indicate possible new *leading order* effects in the standard CKM3 matrix elements due to mixing with the fourth family.

IV. UNEXPECTED PARAMETER REGIONS

In the experimentally allowed regions of the parameter space we typically find regions, where the mixing with the fourth family is very small and the CKM elements of the first three families are close to the minimal standard model values. There are also some allowed regions with large deviations from the standard expectations. In order to clarify the appearing cancellations that veil these unexpected effects in current analyses of the standard CKM matrix, we discuss three sample sets of values for V_{CKM4}. Our three parameter sets read:

	Set I	Set II	Set III
θ_{12}	0.226 606	0.227 264	0.228 225
θ_{23}	0.040 389	0.041 408 3	0.039 522
θ_{13}	0.004 055 9	0.003 821 91	0.003 827 55
θ_{14}	0.027 752 7	0.018 224 8	0.023 289 5
θ_{24}	0.017 655 3	0.078 955 5	0.110 918
θ_{34}	−0.531 735	0.366 353	0.677 976
δ_{13}	3.314 63	0.317 332	1.255 37
δ_{14}	0.925 439	0.283 57	0.502 528
δ_{24}	2.698 29	0.383 156	0.238 529
$m_{t'}$	325.553 GeV	653.842 GeV	389.238 GeV

First we have a look at the CKM elements V_{tx} obtained with these three parameter sets. We give their complex

values, as well as the ratio of their absolute value compared to the SM3 values from [25]:

	Set I	Set II	Set III
V_{td}	0.0212 + 0.0107i	0.0052 − 0.0005i	0.0089 − 0.0059i
$|V_{td}|/|V_{td}^{\text{SM3}}|$	2.72	0.60	1.22
V_{ts}	−0.0391 + 0.0064i	−0.0653 − 0.0109i	−0.0987 − 0.0182i
$|V_{ts}|/|V_{ts}^{\text{SM3}}|$	0.97	1.63	2.47
V_{tb}	0.8609 + 0.0001i	0.9317 − 0.0004i	0.7755 − 0.0006i
$|V_{tb}|/|V_{tb}^{\text{SM3}}|$	0.86	0.93	0.78

These results significantly differ from the values obtained from SM3 CKM fits. In order to clarify the question why these huge effects cannot be seen in the standard CKM fits [44,45] we have a closer look at e.g. Δ_{B_d}. This quantity was defined as

$$\Delta_{B_d} = \frac{M_{12,\text{SM4}}^{B_d}}{M_{12,\text{SM3}}^{B_d}} = \frac{M_{12,\text{SM4}}^{tt,B_d} + M_{12,\text{SM4}}^{(tt'+t't'),B_d}}{M_{12,\text{SM3}}^{B_d}}. \qquad (4.1)$$

The tt part of the SM4 value $M_{12,\text{SM4}}^{tt,B_d}$ looks formally equal to $M_{12,\text{SM3}}^{B_d}$, but the values of the CKM elements V_{tx} can be very different for SM3 and SM4. We further rewrite Δ_{B_d} as

$$\Delta_{B_d} = 1 + \frac{M_{12,\text{SM4}}^{tt,B_d} - M_{12,\text{SM3}}^{B_d}}{M_{12,\text{SM3}}^{B_d}} + \frac{M_{12,\text{SM4}}^{tt'+t't',B_d}}{M_{12,\text{SM3}}^{B_d}}. \qquad (4.2)$$

The first correction term to "1" is due to the difference of the CKM elements V_{tx} in the three and four generation standard model, while the second correction is due to new virtual loop effects of the t' quark. The three parameter sets, discussed in this section, were chosen in such a way

that large cancellations appear mimicking the SM3 perfectly. Therefore, these big effects are invisible in CKM fits. With our special parameter sets we numerically obtain the following values for the three contributions to Δ:

Set I:

$$\Delta_{K^0} = 1 + (0.0139 - 0.0854i) + (-0.0362 + 0.0416i)$$
$$= 0.98 \cdot e^{-i2.5°}, \tag{4.3}$$

$$\Delta_{B_d} = 1 + (-1.6939 - 5.4548i) + (1.7352 + 5.3184i)$$
$$= 1.05 \cdot e^{-i7.5°}, \tag{4.4}$$

$$\Delta_{B_s} = 1 + (-0.3415 + 0.2492i) + (0.3608 - 0.3662i)$$
$$= 1.03 \cdot e^{-i6.5°}, \tag{4.5}$$

$$\Delta_{b \to s\gamma} = 1 - 0.2959 + 0.3715 = 1.0756, \tag{4.6}$$

$$\Phi_s^{\Delta} = -0.114276 = -6.5°. \tag{4.7}$$

Huge cancellations appear, in the case of the imaginary part of B_s mixing up to 500%. Taking experimental and theoretical uncertainties into account, the final results are still perfectly consistent with the SM3 expectation. For the next parameter set we get:

Set II:

$$\Delta_{K^0} = 1 + (-0.0016 - 0.0017i) + (-0.0246 - 0.0071i)$$
$$= 0.97 \cdot e^{-i0.5°}, \tag{4.8}$$

$$\Delta_{B_d} = 1 + (-0.7383 - 0.1732i) + (0.4631 + 0.0826i)$$
$$= 0.73 \cdot e^{-i7.1°}, \tag{4.9}$$

$$\Delta_{B_s} = 1 + (1.2044 - 0.6715i) + (-1.3434 - 0.0354i)$$
$$= 1.11 \cdot e^{-i39°}, \tag{4.10}$$

$$\Delta_{b \to s\gamma} = 1 + 1.3044 - 1.3879 = 0.9165, \tag{4.11}$$

$$\Phi_s^{\Delta} = -0.687 = -39°. \tag{4.12}$$

This set was chosen by looking for large values of Φ_s. As discussed in Sec. II C there are currently some experimental hints for such a deviation from the standard model. Here we confirm the statement from [12] that such a value could be explained by a forth generation of quarks. As a final example we present a parameter set yielding a value for $|V_{tb}|$ as small as 0.78.

Set III:

$$\Delta_{K^0} = 1 + (0.0108 + 0.0919i) + (-0.0388 - 0.0106i)$$
$$= 0.98 \cdot e^{+i4.8°}, \tag{4.13}$$

$$\Delta_{B_d} = 1 + (-0.1691 + 0.3448i) + (0.1681 - 0.4824i)$$
$$= 1.01 \cdot e^{-i7.8°}, \tag{4.14}$$

$$\Delta_{B_s} = 1 + (2.4697 - 1.1837i) + (-2.8227 + 0.8334i)$$
$$= 0.74 \cdot e^{-i28°}, \tag{4.15}$$

$$\Delta_{b \to s\gamma} = 1 + 2.6661 - 2.7172 = 0.9489, \tag{4.16}$$

$$\Phi_s^{\Delta} = -0.4961 = -28°. \tag{4.17}$$

A small value of V_{tb} would also lead to a smaller rate for e.g. the single top production at Tevatron. See e.g. [55] for a recent measurement of this rate.

Note that the effects described in the chosen sets are very sensitive to small variations in the mixing angles and phases of the fourth family. This is obvious as the large cancellations described above require very specific parameter sets. The dependence on the t' mass, in contrast, is moderate.

V. CONCLUSION

We have investigated the experimentally allowed parameter range for a 4×4 quark mixing matrix, making some simplifying assumptions concerning the QCD corrections. Moreover we have not taken into account any correlations with the lepton mixing matrix. As a result we find that the tree-level constraints for the 3×3 CKM matrix and the FCNC bounds from K, D^0, B_d, and B_s mixing as well as the decay $b \to s\gamma$ are typically fulfilled if we have a small mixing with the fourth family, which allows us to perform a Taylor expansion of the 4×4 CKM matrix. Unexpectedly we were also able to find experimentally allowed parameter sets, having a sizable mixing with the fourth generation. In this case also the usual 3×3 CKM matrix elements can change considerably: V_{td} and V_{ts} can differ by up to a factor 3 compared to the SM3 value and V_{tb} can be as low as 0.75; see also [56] for the possibility of V_{tb} being unequal to one. These dramatic effects are not seen in the CKM fits. This is due to large cancellations between the effect of changed matrix elements V_{tx} and effects of virtual heavy b' and t' quarks. An example of such a cancellation was also discussed in [57]. We have also shown that there are parameter ranges consistent with all experimental bounds, which yield large effects for Φ_s. Because of these interesting results, it seems worthwhile to extend the current exploratory analysis. First more flavor observables, like asymmetries, $b \to sl^+l^-$ (see e.g. [58,59]), $B_s \to \mu\mu, \dots$ should be considered. Moreover, the electroweak precision observables have to be included in more detail, here, in particular, the observable R_b seems to be promising; see e.g [60]. Another important improvement will be the exact treatment of the perturbative QCD corrections, in particular, in the decay

$b \to s\gamma$. Finally one also has to take into account correlations to the lepton mixing matrix.

Refined direct measurements of the CKM matrix elements will provide more insight into a possible fourth generation. In particular, future experiments could help to determine the hardly known CKM elements V_{cd} and V_{cs} as well as nonperturbative parameters like form factors and decay constants. Probably the most stringent bounds on the mixing with the fourth generation can be obtained from the direct measurements of V_{td}, V_{ts}, and V_{tb}. V_{tb} is currently investigated at Tevatron; for the latest value of V_{tb} from single top production see [55,61,62]. Also more precise data on FCNC will be very helpful. For the case of

the promising B_s system this is currently done at the Tevatron and in the near future at LHCb [63] and probably at Super B factories [64,65].

[1] P. H. Frampton, P. Q. Hung, and M. Sher, Phys. Rep. **330**, 263 (2000).
[2] G. D. Kribs, T. Plehn, M. Spannowsky, and T. M. P. Tait, Phys. Rev. D **76**, 075016 (2007).
[3] B. Holdom, Phys. Rev. D **54**, R721 (1996).
[4] H. J. F. He, N. Polonsky, and S. f. Su, Phys. Rev. D **64**, 053004 (2001).
[5] V. A. Novikov, L. B. Okun, A. N. Rozanov, and M. I. Vysotsky, Pis'ma Zh. Eksp. Teor. Fiz. **76**, 158 (2002) [JETP Lett. **76**, 127 (2002)].
[6] M. E. Peskin and T. Takeuchi, Phys. Rev. D **46**, 381 (1992).
[7] H. Flacher, M. Goebel, J. Haller, A. Hocker, K. Moenig, and J. Stelzer, Eur. Phys. J. C **60**, 543 (2009).
[8] W. S. Hou, Chin. J. Phys. (Taipei) **47**, 134 (2009).
[9] M. S. Carena, A. Megevand, M. Quiros, and C. E. M. Wagner, Nucl. Phys. **B716**, 319 (2005).
[10] P. Q. Hung, Phys. Rev. Lett. **80**, 3000 (1998).
[11] A. Soni, A. K. Alok, A. Giri, R. Mohanta, and S. Nandi, arXiv:0807.1971.
[12] W. S. Hou, M. Nagashima, and A. Soddu, Phys. Rev. D **76**, 016004 (2007).
[13] A. Arhrib and W. S. Hou, J. High Energy Phys. 07 (2006) 009.
[14] W. S. Hou, M. Nagashima, and A. Soddu, Phys. Rev. Lett. **95**, 141601 (2005).
[15] W. S. Hou, R. S. Willey, and A. Soni, Phys. Rev. Lett. **58**, 1608 (1987); **60**, 2337(E) (1988).
[16] W. S. Hou, A. Soni, and H. Steger, Phys. Rev. Lett. **59**, 1521 (1987).
[17] N. Cabibbo, Phys. Rev. Lett. **10**, 531 (1963).
[18] M. Kobayashi and T. Maskawa, Prog. Theor. Phys. **49**, 652 (1973).
[19] T. Aaltonen et al. (CDF Collaboration), Phys. Rev. D **76**, 072006 (2007).
[20] T. Aaltonen et al. (CDF Collaboration), Phys. Rev. Lett. **100**, 161803 (2008).
[21] P. Q. Hung and M. Sher, Phys. Rev. D **77**, 037302 (2008).
[22] H. Fritzsch and J. Plankl, Phys. Rev. D **35**, 1732 (1987).
[23] H. Harari and M. Leurer, Phys. Lett. B **181**, 123 (1986).
[24] M. Battaglia et al., arXiv:hep-ph/0304132.

[25] C. Amsler et al. (Particle Data Group), Phys. Lett. B **667**, 1 (2008).
[26] T. Inami and C. S. Lim, Prog. Theor. Phys. **65**, 297 (1981); **65**, 1772(E) (1981).
[27] A. J. Buras, M. Jamin, and P. H. Weisz, Nucl. Phys. **B347**, 491 (1990).
[28] S. Herrlich and U. Nierste, Nucl. Phys. **B419**, 292 (1994).
[29] S. Herrlich and U. Nierste, Nucl. Phys. **B476**, 27 (1996).
[30] A. Lenz and U. Nierste, J. High Energy Phys. 06 (2007) 072.
[31] K. Anikeev et al., arXiv:hep-ph/0201071.
[32] A. Lenz, arXiv:0802.0977.
[33] E. Golowich, J. Hewett, S. Pakvasa, and A. A. Petrov, Phys. Rev. D **76**, 095009 (2007).
[34] E. Barberio, R. Bernhard, S. Blyth, O. Buchmueller, G. Cavoto, P. Chang, F. Di Lodovico, H. Flaecher, T. Gershon, L. Gibbons, R. Godang, B. Golob, G. Gomez-Ceballos, R. Harr, R. Kowalewski, H. Lacker, C.-J. Lin, D. Lopes-Pegna, V. Luth, D. Pedrini, B. Petersen, M. Purohit, O. Schneider, C. Schwanda, A. J. Schwartz, J. Smith, A. Snyder, D. Tonelli, S. Tosi, K. Trabelsi, P. Urquijo, R. Van Kooten, C. Voena, and C. Weiser (Heavy Flavor Averaging Group), arXiv:hep-ex/0808.1297.
[35] V. Lubicz and C. Tarantino, Nuovo Cimento Soc. Ital. Fis. **123B**, 674 (2008).
[36] A. Datta and D. Kumbhakar, Z. Phys. C **27**, 515 (1985).
[37] H.-Y. Cheng, Phys. Rev. D **26**, 143 (1982)
[38] I. I. Bigi and N. G. Uraltsev, Nucl. Phys. **B592**, 92 (2001).
[39] E. Golowich and A. Petrov, Phys. Lett. B **427**, 172 (1998)
[40] F. Buccella, M. Lusignoli, and A. Pugliese, Phys. Lett. B **379**, 249 (1996).
[41] J. F. Donogue, E. Golowich, B. R. Holstein, and J. Trampetic, Phys. Rev. D **33**, 179 (1986).
[42] L. Wolfenstein, Phys. Lett. **164B**, 170 (1985).
[43] T. Yanir, J. High Energy Phys. 06 (2002) 044.
[44] C. Tarantino, arXiv:0902.3431.
[45] A. Hocker, H. Lacker, S. Laplace, and F. Le Diberder, Eur. Phys. J. C **21**, 225 (2001).
[46] M. Beneke, G. Buchalla, C. Greub, A. Lenz, and U. Nierste, Phys. Lett. B **459**, 631 (1999).
[47] M. Beneke, G. Buchalla, A. Lenz, and U. Nierste, Phys.

Lett. B **576**, 173 (2003).

[48] M. Ciuchini, E. Franco, V. Lubicz, F. Mescia, and C. Tarantino, J. High Energy Phys. 08 (2003) 031.

[49] E. Barberio *et al.* (Heavy Flavor Averaging Group), http://www.slac.stanford.edu/xorg/hfag/.

[50] T. Aaltonen *et al.* (CDF Collaboration) CDF Public Note 9458; T. Aaltonen *et al.* (CDF Collaboration), Phys. Rev. Lett. **100**, 161802 (2008); **100**, 121803 (2008); V. M. Abazov *et al.* (D0 Collaboration), Conference Note 5730-CONF; V. M. Abazov *et al.* (D0 Collaboration), Conference Note 5618-CONF; V. M. Abazov *et al.* (D0 Collaboration), Phys. Rev. D **76**, 057101 (2007); Phys. Rev. Lett. **98**, 121801 (2007).

[51] O. Deschamps, arXiv:0810.3139.

[52] J. Charles, Nucl. Phys. B, Proc. Suppl. **185**, 17 (2008).

[53] L. Wolfenstein, Phys. Rev. Lett. **51**, 1945 (1983).

[54] A. J. Buras, M. E. Lautenbacher, and G. Ostermaier, Phys. Rev. D **50**, 3433 (1994).

[55] T. Aaltonen *et al.* (CDF Collaboration), Phys. Rev. Lett. **100**, 161803 (2008).

[56] J. Alwall *et al.*, Eur. Phys. J. C **49**, 791 (2007).

[57] W. S. Hou, M. Nagashima, and A. Soddu, Phys. Rev. D **72**, 115007 (2005).

[58] T. M. Aliev, A. Ozpineci, and M. Savci, Nucl. Phys. **B585**, 275 (2000).

[59] G. Buchalla, G. Hiller, and G. Isidori, Phys. Rev. D **63**, 014015 (2000).

[60] P. Bamert, C. P. Burgess, J. M. Cline, D. London, and E. Nardi, Phys. Rev. D **54**, 4275 (1996).

[61] V. M. Abazov *et al.* (D0 Collaboration), arXiv:0903.0850.

[62] T. Aaltonen *et al.* (CDF Collaboration), arXiv:0903.0885.

[63] LHCb Collaboration, JINST **3**, S08005 (2008).

[64] M. Bona *et al.*, arXiv:0709.0451.

[65] S. Hashimoto *et al.*, Report No. KEK-REPORT-2004-4.